Carbohydrate Polymers 136 (2016) 1041–1051

Contents lists available at ScienceDirect

Carbohydrate Polymers

journal homepage: www.elsevier.com/locate/carbpol

Carrot fiber (CF) composite films for antioxidant preservation: Particle size effect

Alondra M. Idrovo Encalada[a,b], Maria F. Basanta[a,c], Eliana N. Fissore[a,c], Maria D. De'Nobili[a,c], Ana M. Rojas[a,c,*]

[a] Departamento de Industrias, Facultad de Ciencias Exactas y Naturales, University of Buenos Aires, Argentina
[b] SENESCYT, Ecuador
[c] National Research Council of Argentina (CONICET), Argentina

ARTICLE INFO

Article history:
Received 19 July 2015
Received in revised form
13 September 2015
Accepted 30 September 2015
Available online 9 October 2015

Keywords:
Carrot fiber
Average particle size
Composite films
Pectins
Carotenoids and phenolics
Antioxidant preservation

ABSTRACT

The effect of particle size (53, 105 and 210 μm) of carrot fiber (CF) on their hydration properties and antioxidant capacity as well as on the performance of the CF-composite films developed with commercial low methoxyl pectin (LMP) was studied. It was determined that CF contained carotenoids and phenolics co-extracted with polysaccharides (80%), rich in pectins (15%). CF showed antioxidant activity and produced homogeneous calcium–LMP-based composites. The 53-μm-CF showed the lowest hydration capability and produced the least elastic and deformable composite film due probably to CF bridged by calcium-crosslinked LMP chains. Antioxidant activity associated to the loaded CF was found in composites. When L-(+)-ascorbic acid (AA) was also loaded, its hydrolytic stability increased with the decrease in CF-particle size, showing the lowest stability in the 0%-CF- and 210 μm-CF-LMP films. Below ≈250 μm, the particle size determined the hydration properties of pectin-containing CF, affecting the microstructure and water mobility in composites.

1. Introduction

Carrot (*Daucus carota* L.) is one of the important root vegetables rich in bioactive compounds like carotenoids and dietary fibers with appreciable levels of several other functional components having significant health-promoting properties. The phytonutrient content of carrots also includes phenolics and polyacetylenes. Carrot is rich in β-carotene, L-(+)-ascorbic acid (AA) and tocopherol and is classified as a vitaminized food (Hashimoto & Nagayama, 2004). In Argentina, fruit and vegetable processing is the activity that originates the highest amount of organic residues (Ministerio de Agricultura, Ganadería, Industria y Comercio de la Provincia de Santa Fe, 1999). Carrot roots, with a variable volume of production, originate 20–80 Tn/day of by-products or wastes which are not industrialized but used for animal feed. Carrots are discarded because of no adequate size and/or shape for commercialization, or because the economical value is not enough to justify the spending in harvesting and transport (Sánchez & Cardona, 2008). They can be an alternative carbon source and applied to the extraction of fibers used for material development such as composite films. Edible films are much studied matrices since they can be applied as a technological hurdle for food preservation because their microstructure can be used to carry, stabilize, localize the activity and control the release of food preservatives (antimicrobials, antioxidants) at interfaces. Edible films habitually developed for food protection are very good barriers to gases but not to water vapor because polysaccharides and proteins have to be used for their development. Composite films can be obtained by loading fibers of vegetable origin such as fruit-puree or cellulose, to modify the mechanical and barrier properties of films (Huq et al., 2012; Valencia-Chamorro, Palou, del Río, & Pérez-Gago, 2011). Alginate–apple puree films with essential oils of oregano, or lemongrass/citral as well as of cinnamon were developed for antimicrobial protection of food (Rojas-Graü et al., 2007). Azeredo, Miranda, Rosa, Nascimento, and de Moura (2012) developed alginate based films with the addition of acerola puree as well as of cellulose whiskers obtained from cotton fiber and treated coconut husk fiber with the objective of modify the mechanical and water vapor permeability (WVP). Research works about film development with loading of nanoparticles are developed to investigate the concentration effect of nanoparticles of a given particle size range on the barrier and mechanical properties of films (Abdollahi, Alboofetileh, Rezaei, & Behrooz, 2013; Huq et al., 2012; Sirviö, Kolehmainen, Liimatainen, Niinimäki, & Hormi,

* Corresponding author at: Departamento de Industrias, Facultad de Ciencias Exactas y Naturales, University of Buenos Aires, Argentina.
E-mail address: arojas@di.fcen.uba.ar (A.M. Rojas).

http://dx.doi.org/10.1016/j.carbpol.2015.09.109
0144-8617/

2014). Abdollahi et al. (2013) used alginate to produce by casting nanocomposite films containing cellulose nanowhiskers (1–10% w/w on solid sodium alginate) produced by sulfuric acid hydrolysis of microcrystalline cellulose (10–15 μm). In these works is in general determined that an ideal particle concentration exists where the WVP is minimal and the tensile strength is maximal, though accompanied by the lowest film deformability.

Vegetable fibers, which are essentially constituted by the cell wall polysaccharides, are isolated with co-extracted natural antioxidants (e.g. phenolics) associated to the polysaccharides. Also, β-carotene, which is coming from the vegetable cells. It is then suggested that the extracted CF may constitute the natural polymeric matrix for supporting of phenolics and β-carotene. AA can protect β-carotene from bleaching while contributes to the antioxidant activity. Together with AA, the antioxidant active CF can then be applied to the development of composite films for food preservation, with simultaneous modification of the film performance (mechanical properties and WVP). Also, the edible film matrix can stabilize the loaded active compounds, control their delivery and localize the antioxidant activity at food interfaces (De'Nobili, Rojas, Abrami, Lapasin, & Grassi, 2015). However, it is proposed that the particle size of CF can affect the hydration properties of fibers and, hence, the film performance and the life-time as antioxidant active interface. In view of the above mentioned, the aim of the present work was to determine the effect of the particle size of CF isolated from root residues on its hydration properties and performance of the antioxidant composite films based on commercial low methoxyl pectin (LMP), also loaded with AA. The relation between hydration properties of CF and composite film performance was analyzed.

2. Materials and methods

2.1. Chemicals

They were from Sigma–Aldrich (Saint Louis, USA) and Merck Química (Argentina). Food grade pectin with a low degree of methyl esterification (GENU™ pectin type LM-12 CG) for manufacturing foodstuffs was a gift from CP Kelco (Denmark). Deionized water (Milli-Q™, USA) was used.

2.2. Fiber extraction

Carrot (*Daucus carota* L.) roots were those harvested and discarded because of irregular sizes (Mendoza, Argentina). The remnant of leaves and the stem were eliminated as a slice from each carrot. Carrots were cleaned carefully with detergent, rinsed with tap water and finally with distillate water, and left for draining. Roots were cut into dices and juice was extracted (Moulinex, France). The solid residue was separated from the extractor machine and suspended in deionized water (4:1 v/w, water:vegetable) at room temperature, under stirring, after which the suspension was filtrated though a plastic sieve, being recovered the solid residue while the aqueous phase was discarded. This washing process was repeated three times more in order to eliminate the water soluble substances like sugars. Finally, a fifth extraction was performed under stirring with deionized water at a constant temperature of 90 °C during 5 min for enzyme inactivation. This final residue obtained was cooled by immersion in 6 °C-deionized water, sieved, drained and frozen in liquid nitrogen and freeze-dried (Christ, Germany; Pfeiffer vacuum pump, Germany).

The carrot fiber obtained was milled in a cutting mill (Wemir, Argentina) and the total powder obtained was mixed, weighed and sieved through a vibratory sieve shaker (Retsch, Germany) provided with a series of six ASTM mesh sizes of 840, 420, 210, 105, 53 and 25 μm. Each powder fraction recovered between the two closest sieves was weighed in order to calculate the yield of powder corresponding to each average particle size. Powder fractions were separately distributed between small Cryovac bags (USA), sealed under vacuum (Multivac C-200, Germany), and each bag was wrapped in aluminum foil for darkness, and stored in freezer at −20 °C until usage.

2.3. Water activity

Water activity (a_W) of CF (53, 105 and 210 μm average particle sizes) and film samples was evaluated in triplicate at 25.0 °C through a Decagon AquaLab (Series 3 Water activity meter, USA), by measurement of the relative humidity (RH) of the air in equilibrium (ERH) with the sample (Eq. (1)). A calibration curve made by measuring saturated solutions of known a_W° [LiCl ($a_W^\circ = 0.110$), CH_3COOK ($a_W^\circ = 0.220$), $MgCl_2$ ($a_W^\circ = 0.333$), NaBr ($a_W^\circ = 0.577$) and NaCl ($a_W^\circ = 0.752$), at 25.0 °C (Greenspan, 1977)] was used to extrapolate a_W° from the a_W value read in the equipment.

$$a_W = \frac{ERH}{100} \quad (1)$$

2.4. Moisture

The water content of carrot fibers as well as of cut films was determined by drying under vacuum at 70 °C up to constant weigh (≈22 d) into an oven (Gallenkamp, UK). The results were calculated per 100 g of dry mass.

2.5. Chemical analyses

Total phenolics were determined through the Folin–Ciocalteau's spectrophotometric technique after alkaline hydrolysis of sample, as reported by Basanta, de Escalada Pla, Stortz, and Rojas (2013). Results were expressed as mg of gallic acid per 100 g of dried sample. Carotenes were determined according to the spectrophotometric method described by Biswas, Sahoo, and Chatli (2011), using β-carotene as standard.

Cellulose, lignin and non-cellulosic polysaccharides were separated with sulphuric acid-aqueous solutions (1 M or 72% v/v), as explained by Basanta et al. (2013).

When corresponded, the following analyses were performed, as reported by Basanta et al. (2013): uronic acids, total carbohydrates of polysaccharides, protein content (bovine serum albumin as standard) and total starch, which was determined through an enzymatic method involving α-amylase, amyloglucosidase and *o*-dianisidine (Karkalas, 1985), using the reactive solutions prepared according to a kit before provided by Sigma (USA). The neutral sugar content was calculated as the arithmetical difference between the non-cellulosic polysaccharide and the uronic acid contents.

2.6. Antioxidant capacity

It was determined through the radical scavenging activity of the carrot fiber or cut film samples by using the DPPH (2,2-diphenyl-1-picrylhydrazyl) assay (Brand-Williams, Cuvelier, & Berset, 1995). Also, through the ferric reducing antioxidant power (FRAP) assay reported by Benzie and Strain (1996) and Pulido, Bravo, and Saura-Calixto (2000). Samples were extracted with methanol and results were expressed on L-(+)-ascorbic acid (AA) as the standard in both methods, whose calibration curves were developed with the standard dissolved in methanol.

2.7. Color

Fiber color was put into a 20-mm-diameter transparent and colorless cell. In the case of films, the exposed area was sufficiently large in relation to the illuminated area to avoid any edge effect (Trezza & Krochta, 2000). Color was measured with a Minolta colorimeter (Minolta CM-508d, Japan) provided with an aperture of 1.5 cm-diameter, at ten different points across the sample surface. Hunter Lab color parameters [L = 0% (black) and L = 100% (white or maximum) for lightness, $-a$ (greenness) and $+a$ (redness), $-b$ (blueness) to $+b$ (yellowness)] were determined using the D65 standard illuminant and the 2° standard observer. The average and standard deviation for the triplicates of fiber or film samples was reported.

2.8. Hydration and physical properties

Swelling capacity (SC), water holding capacity (WHC), water retention capacity (WRC) and kinetic of spontaneous water absorption were determined for the extracted carrot fibers in triplicate, as described by Basanta et al. (2013). Data of spontaneous water absorption were fitted to a power-law relationship for swelling according to Ritger and Peppas (1987):

$$q = k \cdot t^n \tag{2}$$

where q (mL/g) corresponds to the water absorbed at time t, k is a constant dependent on kinetic features and experimental conditions, and n is the swelling exponent.

Mean values and standard deviation of three measurements for each fraction were reported.

The specific volume (SV) was determined according to Chau, Wang, and Wen (2007) and the apparent density (g/cm^3) was the inverse of SV. True density was measured as indicated by de Escalada Pla, Uribe, Fissore, Gerschenson, and Rojas (2010). Porosity (Pr) was then calculated as:

$$Pr = \left[1 - \left(\frac{\rho_{\text{bulk}}}{\rho_{\text{true}}}\right)\right] \times 100 \tag{3}$$

Mean values and standard deviation of ten measurements for each fraction were reported.

2.9. Fast Fourier transform infrared spectroscopy (FTIR)

Transmission spectra of the fiber samples were recorded from KBr (1% w/w) pellets, whereas the spectra of film samples were recorded with a diamond attenuated total reflection (ATR) device, a DTGS TEC detector, and a reflection incident angle of 45°, with a Nicolet 8700 (Thermo Scientific Nicolet, MA, USA) spectrometer as described by Pérez, Flores, Marangoni, Gerschenson, and Rojas (2009).

2.10. Filmmaking procedure

Four systems were prepared: (a) film without carrot fiber (0% fiber-LMP), and LMP-composite film loaded either with (b) 53 μm-, (c) 105 μm-, or (d) 210 μm-fiber.

CF (0.4000 g) of a given average particle size (53, 105 or 210 μm) was dispersed in 30.00 mL of deionized water, mixed slightly through a vortex for complete humectation and left for 18 h at 25 °C for hydration.

The film making solution was made into a glass beaker containing ≈250.00 g of deionized water, where 8.00 g of the commercial GENU™ pectin, which contained 5.25 g of low methoxyl pectin (LMP), was slowly poured under continuous controlled high-speed shear (1400 rpm-constant) stirring performed with a vertical stirrer (LH, Velp Scientifica, Italy), in order to reach homogeneous hydration of the powder without lumps. After heating to 90 °C (5 °C/min), potassium sorbate and AA were added, as explained by De'Nobili, Pérez, Navarro, Stortz, and Rojas (2013), and 4.00 g of glycerol were herein used for plasticization (0.762 g/g LMP). The 30 mL of CF dispersion were then added to the film making solution while stirring, followed by the addition of 0.500 g of $CaCl_2.2H_2O$ pre-dissolved in 3 mL of water, while maintaining the system stirred (85 °C). Total weight of the film making solution was then completed to 300.00 g by addition of enough deionized water, followed by homogenization (De'Nobili, Pérez, et al., 2013). The pH of the solution was 3.12. This hot solution was placed under vacuum for 20 s to remove air bubbles and poured (≈9.0000 g, analytical scale) onto each horizontally leveled and numbered polystyrene plate (55-mm diameter). It is then known the initial content of AA [called "$weight_{AA}(o,loaded)$"; Eq. (4)] into each subsequently generated film. Once cooled to room temperature for gelling, drying was performed (60 °C, 3 h) under forced convection. Films were left for cooling, peeled off and stored under vacuum into a light-protected desiccator (26-cm-diameter Nalgene, USA) at 25.0 °C, over a saturated solution of NaBr ($a_W^\circ = 0.577$), in order to maintain a constant RH (57.7%) for film equilibration (Eq. (1)) (Greenspan, 1977).

Three batches of films (triplicate) for each of the four systems studied were produced as explained. The AA content was then measured at initial time (t = 0) as well as during film storage (time -t-) in each of the three films taken from each batch of a given system, by using the spectrophotometric technique reported by De'Nobili, Curto, et al. (2013). This AA content measured was called "$weight_{AA}(t)$" (Eq. (4)). Hence, the AA proportion remaining at any time [$C_{AA}(t)$] (Eq. (4)), including t = 0, can be calculated as follows:

$$C_{\text{AA}}(t) = \frac{weight_{\text{AA}}(t)}{weight_{\text{AA,film}}(o,\ loaded)} \tag{4}$$

where $C_{\text{AA}}(t=0) = \frac{weight_{AA}(o)}{weight_{AA,film}(o,loaded)} = 1.00$

2.11. Water vapor permeability (WVP) of films

It was determined following the procedure and calculations indicated by Gennadios, Weller, and Gooding (1994) for hydrophilic films, by taking into account the resistance of the air column to the vapor transference in the space (10 mm in height) remaining between the anhydrous calcium chloride desiccant placed into the cup and the film sample at the top of the beaker, which was in contact with an environment of 73% RH at 25 °C (Ibertest chamber, Spain).

2.12. Atomic force microscopy (AFM)

This study was performed on film samples under a nitrogen atmosphere, by taking images with a cantilever through an atomic force microscope (NanoScope III, Digital Instruments, CA) and performing image analysis (Horcas, Fernandez, Gomez-Rodriguez, and Colchero, 2007) with the scanning probe microscopy software WSxM 4.0 Develop 11.3-Package (2007, Nanotec Electronica, Spain), as previously indicated (León et al., 2009).

2.13. Contact angle

Contact angle was tested through the sessile drop (0.0040 mL) deposited at three representative areas of each horizontally leveled film surface (three films for each of the four systems studied) using a contact angle goniometer (NRL Contact Angle Goniometer, model 100–00, Rame-Hart, USA) provided with a magnifying glass (Nikon, SMZ-2T, Japan). A drop of deionized water was dispensed using a micrometer syringe (Gilmont Instruments, Cole-Parmer, USA). At 5 and 60 min of the drop deposition, an image was taken with a digital Nikon camera (COOLPIX 950, Japan) and processed with Corel

Draw 9.0 package (Designer.com, USA), which permitted the measurement of the angle between the horizontally fitted base of the drop image and the tangent line drawn.

2.14. Tensile assays

Each film sample strip (25.0 mm × 6.0 mm) was submitted to a mechanical test under static, transient conditions in the uniaxial tensile mode, at 25.0 °C, using a controlled stress DMA (Q 800, TA Instruments, New Castle, DE, USA), equipped with tension clamps. One end of the strand was attached to a superior mobile clamp and the other end attached to a lower fixed clamp, leaving a 12 mm-gap. A preload force of 10^{-2} N and a constant force ramp of 0.3 N/min were applied to record the stress (σ) vs strain (ε) curves until rupture from the film sample strips. At least four replicates for each film system were measured.

In order to determine the elastic modulus of films, the acquired curves were analyzed. The elastic modulus could be evaluated as the slope of the stress–strain curve, initially, at the linear low strain region. Therefore, the stress–strain curves were firstly transformed into the true stress–true strain curves, and then the elastic modulus was calculated by fitting the following mathematical model to the whole true tensile stress–true strain curves:

$$\sigma_T(\varepsilon_T) = E_C \cdot \varepsilon_T \cdot \exp(\varepsilon_T \cdot K) \quad (5)$$

where σ_T and ε_T are the true stress and true strain, respectively, calculated according to Mancini, Moresi, and Rancini (1999) [Eqs. (6) and (7)]; E_C is the elastic modulus (i.e. the tangent to the stress-strain curve at the origin); K is a constant and it was regarded as a fitting parameter (Del Nobile et al., 2007).

$$\sigma_T = \sigma(1 - \varepsilon) \quad (6)$$

$$\varepsilon_T = -\ln(1 - \varepsilon) \quad (7)$$

The modulus of rupture (E_{rupt}) or strength was also reported after calculation of the relation between the ultimate properties, that is, the stress (σ) and strain (ε) at the moment of film rupture.

$$E_{rupt} = \frac{\sigma_{rupt}}{\varepsilon_{rupt}} \quad (8)$$

2.15. Glass transition temperature (T_g)

Modulated differential scanning calorimetry (MDSC, TA Instruments, USA) was used to determine the T_g (midpoint temperature) from the second scan performed on an equilibrated film sample (10–15 mg), as described by De'Nobili, Pérez, et al. (2013).

2.16. Statistical analysis

Results were informed as the average and standard deviation for n replicates of each sample, after analyzed through ANOVA (level of significance, $\alpha = 0.05$) followed by multiple comparisons evaluated through the least significant difference test, using the Statgraphic package (Statgraphic Plus for Windows, version 5.0, 2001, Manugistic Inc., USA).

Rate constant of AA hydrolysis (k'_{AA}) was calculated by linear regression according to a first order reaction, where AA concentration was expressed as indicated in Eq. (4) [$C_{AA}(t)$]. Analysis of covariance (ANCOVA) was applied for comparison of slopes, that is, of the rate constants (k'_{AA}), as indicated by Sokal and Rohlf (2000). The half-life times ($t_{1/2}$) were calculated according to a one-order kinetic and a stoichiometric coefficient $\nu_i = 1$:

$$t_{1/2} = \frac{0.693}{\nu_i \cdot k'_{AA}} \quad (9)$$

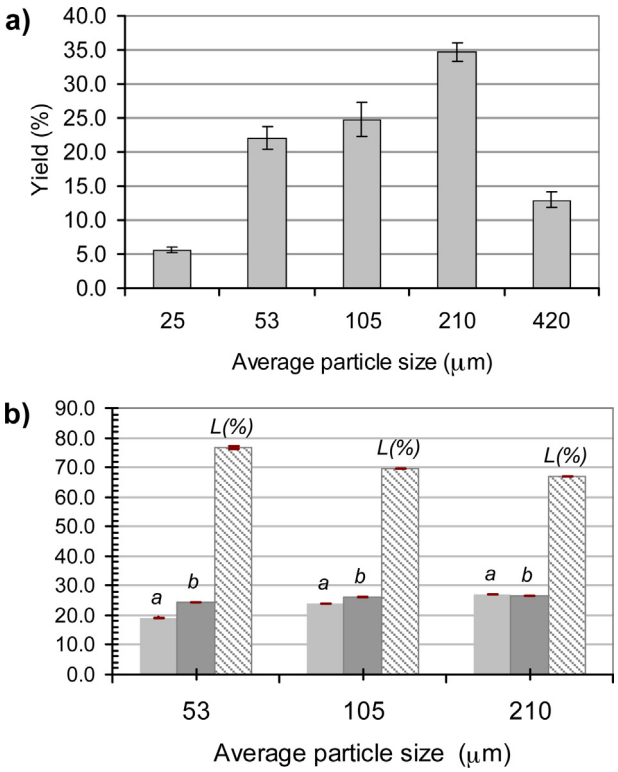

Fig. 1. Yield in average particle sizes of carrot fiber (a). Hunter Lab color parameters (a, b and lightness, L%) of carrot fibers plotted against the average particle size (b). Error bars correspond to the standard deviation ($n = 3$; $n > 12$ for color parameters).

3. Results and discussion

3.1. Carrot fibers

The dried and milled fiber isolated from carrot was obtained by applying a final extractive step in water at high temperature (90 °C) to achieve enzyme inactivation. The highest yield (22–35%) of the fiber powder was respectively obtained for fractions of 53, 105 and 210 μm of average particle sizes, and lower proportions for 25 and 420 μm (Fig. 1a). Hence, fibers with average particle sizes of 53, 105 and 210 μm were selected as particulate filler material for the development of composite-LMP edible films. In order to know the properties of this natural fiber used in the material development, the chemical composition and hydration properties were first determined as a function of the particle size. The CF showed a water activity (a_W°) ranging 0.356–0.397 (Table 1), which was low enough to prevent the fiber powder from microbial spoilage and chemical degradation during storage (Labuza, McNally, Gallagher, Hawkes, & Hurtado, 1972).

3.1.1. Color

Hunter Lab color space parameters obtained from the CF are shown in Fig. 1b. The a and b values were both above zero, between +20 and +30, intersecting points in the red–yellow color space (Fig. 1b). The a and b values increased significantly ($p < 0.05$) with the particle size, shifting to redder and more yellow color, respectively. The high values of lightness (L) obtained for CF decreased significantly ($p < 0.05$) (color darkening) from 76% to 67% when the particle size increased (Fig. 1b).

3.1.2. Chemical composition

As reported in Table 1, the 53, 105 and 210 μm CF were the water insoluble residues, essentially enriched in cell wall polysaccharides, with a 62–67% of non-cellulosic polysaccharides (neutral

Table 1
Chemical composition,[a] antioxidant capacity[a,b] as well as the Ritger and Peppas' model parameters[b] obtained from carrot isolated fibers.

	Average particle size (μm)		
	53	105	210
Water activity (21.0 °C)	0.397 ± 0.002	0.356 ± 0.003	0.370 ± 0.002
Neutral sugars (% w/w)	50.9 ± 0.05	50.8 ± 0.04	47.0 ± 0.08
Uronic acids (% w/w)	15.8 ± 0.8	14.3 ± 0.02	15.0 ± 0.02
Cellulose (% w/w)	23.5 ± 0.7	25.6 ± 0.8	25.1 ± 0.6
Lignin (% w/w)	7.1 ± 0.8	7 ± 1	10 ± 2
Total starch (% w/w)	0.69 ± 0.09	0.72 ± 0.05	0.71 ± 0.07
Proteins (% w/w)	2.7 ± 0.2	2.3 ± 0.2	2.4 ± 0.3
Total polyphenol content (mg GA/100 g fibers)	241 ± 27	232 ± 3	246 ± 18
Total carotenoid content (mg/100 g fibers)	18.62 ± 0.02	17.10 ± 0.04	17.08 ± 0.01
DPPH (mg AA/100 g fiber)	33 ± 2	29 ± 1	27 ± 1
FRAP (mg AA/100 g fiber)	25.8 ± 0.2^{A}	29 ± 3^{B}	25.6 ± 0.6^{AB}
k (mL g^{-1} s^{-1})[b]	5.4 ± 0.4	8.1 ± 0.6	8.8 ± 0.6
N (exponent)[b]	0.19 ± 0.01	0.16 ± 0.01	0.15 ± 0.01
R^2	0.938	0.918	0.907

[a] Mean and standard deviations for $n = 3$ are reported.
[b] Results of the DPPH and FRAP assays are expressed as L-(+)-ascorbic acid (AA).
GA: galic acid.
R^2 values of the nonlinear regression fitting to the Ritger and Peppas' model are also reported.

sugars + uronic acids), 23–25% of cellulose, 7–10% of lignin and ≈0.72% of total starch. About 2.5% of proteins and a total polyphenol content of ≈240 mg, expressed as galic acid per 100 g of dry fibers, remained in the CF (Table 1). Oviasogie, Okoro, and Ndiokwere (2009) reported a coincident total phenolic content of 27 μg/g in carrots, determined on a methanolic extract. The presence of 8–8′ (aryl tetralin form)-dehydrodiferulic acid in carrot cell walls may have a special role in cell–cell adhesion of carrot root tissue, which are hydrolyzed in the alkaline medium (Waldron, Smith, Parr, Ng, & Parker, 1997). On the other hand, a total carotenoid content of ≈17 mg/100 g dry fiber (Table 1) was determined in the isolated CF, which was responsible for the fiber color (Fig. 1b). Frias, Peñas, Ullate, and Vidal-Valverde (2010) found a β-carotene content of 43.87 mg/100 g dry matter in raw carrots. Hence, a lower but significant proportion of carotenes remained in the herein isolated fiber after extraction (Table 1). In reference to the protein content, a hydroxyproline-rich cell wall protein was found by van Holst and Varner (1984) in the cell wall of carrot roots.

As demonstrated by the uronic acid content (≈15% w/w), part of the non-cellulosic polysaccharides included pectins (Table 1). The neutral sugars, which constitute the rest of the non-cellulosic polysaccharides (≈47–51% w/w) (Table 1), can be in part ascribed to the rhamnogalacturonan I domain of pectin macromolecules (rhamnose, galactose and arabinose) (Vincken et al., 2003) and to the neutral sugars that constituted hemicelluloses (Scheller & Ulvskov, 2010).

As determined, the chemical composition was independent of the particle size and, hence, the mechanical milling process did not favor a differential distribution of the polymeric components. On the other hand, the CF pectins can swell during hydration in the film forming solution and contribute to the formation of the film network basically developed by the commercial LMP. Also, CF pectins can show some different capacity of water adsorption into the films.

3.1.3. Antioxidant capacity

The antioxidant capability of CF was evaluated as their radical scavenging (DPPH assay) and reducing (FRAP assay) activities. Both of them were expressed on the AA basis. As shown in Table 1, the

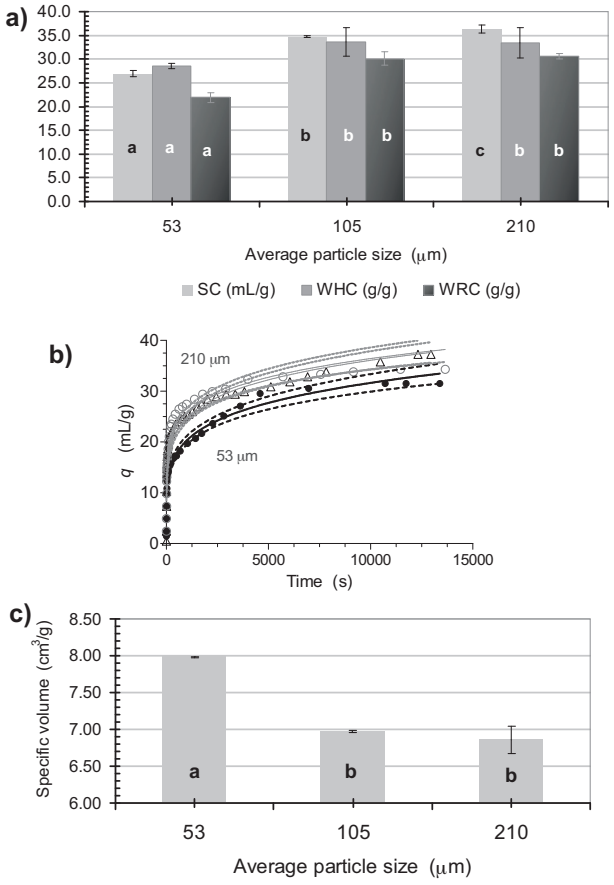

Fig. 2. Swelling (SC), water holding (WHC) and water retention (WRC) capacity of carrot fibers plotted against the average particle size (a). Kinetic curves of spontaneous water absorption by 53 (●), 105 (△) and 210 μm (○) fibers are shown, with the Ritger and Peppas' equation fitting (continuous lines) (b). Specific volume reported against the particle size (c). The same lower case letters for a given property indicates non-significant differences ($p < 0.05$). Error bars correspond to the standard deviation ($n = 3$).

radical scavenging activity of CF was equivalent to ≈30 mg of AA per 100 g of dry fiber powder and tended to decrease with the rise in particle size, while the reducing activity of Fe(III) was equivalent to 25.6–29 mg of AA per 100 g of fiber. The antioxidant capacity may in part be ascribed to the content of carotenoids like β-carotene (Table 1). When protected from light, singlet oxygen quenchers such as β-carotene also function as preventive inhibitors of oxidation. Conjugated polyene system of carotenoids has been found to interact with peroxyl radicals (Gordon, 2001). The phenolic content (Table 1) can be also decisive in the antioxidant capacity shown by CF. Sharma, Karki, Thakur, and Attri (2012) reported that phenolics could play an important role in the antioxidant properties of carrots.

3.1.4. Hydration properties

Since the CF herein obtained were applied to film development, it was considered as necessary to determine if the particle size affected their hydration properties, which are associated to the functional performance of vegetable fibers. Hence, the hydration properties of CF can affect the final performance of films. Hydration properties such as SC increased significantly ($p < 0.05$) with the particle size of the CF from 26.7 mL of water absorbed after 18 h of equilibration per gram of dried fiber, up to 36.3 mL/g for 210 μm (Fig. 2a). Pectins present in the CF (Table 1) are mainly responsible for the water absorption and swelling capacity (Basanta et al., 2013). The values of WHC and WRC determined as the grams

of water absorbed by the dried fibers after 18 h of equilibration per gram of fiber, were significantly lower for 53-μm CF than for 105 and 210 μm (Fig. 2a). Cadden (1987) also observed that reducing the particle size of wheat bran decreased the WHC, which was explained as due in part to the collapse of the fiber matrix by milling. However, the particle size showed less effect on the WHC of microcrystalline cellulose. On the other hand, Rhagavendra, Rastogi, Raghavarao, and Tharanathan (2004) determined that the reduction in the particle size of coconut grating residue from 1127 to 550 μm, resulted in increased hydration properties (SC, WHC and WRC), which was ascribed to the increase in the theoretical surface area and total pore volume, as well as to an structural modification. However, below 550 μm, the hydration properties were found to decrease with decreasing particle size.

The kinetic curve of spontaneous water absorption by the CF from a reservoir was also lower for the 53 μm powder than for 105 and 210 μm of average particle size (Fig. 2b). Therefore, the rate constant of water absorption (k) obtained by fitting of the Ritger and Peppas (1987) model (Eq. (2)) was the lowest for the 53-μm fiber powder, though the influence of the time variable (t) was slightly different, since the exponent decreased (n = 0.19–0.15) with the particle size (Table 1). The maximum amount of water that the fiber can hold is a function of its chemical, physical and microstructural characteristics (Brett & Waldron, 1996; Rhagavendra et al., 2004). Considering all the hydration results, the milling of CF to a 53 μm average particle size seems to diminish the hydrophilic behavior. The chemical composition of CF was not different for the three particle sizes studied (Table 1). It is then thought that the different hydration properties can be related with the fiber microstructure. In this sense, the specific volume was significantly ($p < 0.05$) higher for 53 μm carrot fiber (8 cm^3/g) than for 105 and 210 μm powders (Fig. 2c). The specific volume (cm^3/g) can be used as an indicator of the differences in capillary structure. Theoretically, the most porous the system is, the greater amount of water should be taken up, assuming the chemical composition remains the same. However, it should be taken in mind that the SV assay herein performed measured not only the porosity of each microparticle but also the porosity of the bed formed by the fiber powder particles after tapping. Actually, the 53 μm particle size fiber was lighter than 105 and 210 μm fiber particles. The apparent density of the carrot fiber increased significantly from 0.125 g/cm^3 for 53 μm to 0.146 g/cm^3 for 105 and 210 μm of average particle size. On the other hand, the true density or density of the solid matrix, excluding the pores as well as the void spaces between particles within the bulk sample, was in general non significantly ($p < 0.05$) dependent on the average particle size, with values of 1.60 (±0.05) g/cm^3 for 53 μm and 1.54 (±0.04) g/cm^3 for 105 and 210 μm. A similar porosity of CF was then calculated (Eq. (3)), being 92.17% for 53 μm and 90.68–90.47% for 105 and 210 μm, respectively. The drying procedure always affects the microstructural characteristics of the powders obtained (Vetter & Kunzek, 2003). Considering all the hydration results, the isolated carrot fibers were more or less hydrophilic and then can be compatible as fillers with the LMP used for film development. Also, the milling of CF to 53 μm diminished the water absorption capacity of fiber.

3.2. Antioxidant composite films

Films were developed with commercial LMP by using calcium ion (6.48×10^{-4} mol Ca^{2+}/g pectin) for crosslinking and glycerol (76.2 g/100 g pectin) for plasticization. Films without loading of CF (0%-CF LMP) were obtained for comparison. On the other hand, composite films were developed by loading CF (7.6 g/100 g pectin polymer) of each average particle size (53, 105 and 210 μm), as filler of the LMP network. This fiber concentration was selected through a previous assay in order to obtain handling films. AA was also loaded besides CF. The 0%-CF-LMP film and the composites studied were equilibrated by storage at constant temperature (25.0 °C) and relative humidity (RH = 57.7%) (Eq. (1)), reaching the equilibrium with the environment at about 48 h for the LMP films and 5–6 days for the composite films. Film thickness was then measured, being observed that in general increased significantly ($p < 0.05$) with the fiber particle size (Table 2), for the same weight of film forming solution distributed among plate dishes. It was ascribed to the increase in the film volume because of the increase in the CF particle size.

3.2.1. Moisture content and glass transition temperature (T_g)

As observed in Table 2, the moisture content of film and composites determined after their equilibration (57.7% RH) was not significantly different (≈25.5 g/100 g dry mass). Macromolecular relaxation or mobility determined in the equilibrated films was not very different between systems, as observed from the similar values of T_g obtained, which were between −68.49 °C and −72.34 °C (Table 2). At the same level of moisture content (Table 2), glycerol plasticization was responsible for these low T_g values, together with the water adsorbed after film equilibration at 57.7% RH (León & Rojas, 2007). Since the T_g values were below the room temperature, the films were at the amorphous rubbery state at this environmental condition. Similar values of change in specific heat at the glass transition, expressed on dry mass, were also observed (≈3.5 $J\,g^{-1}\,K^{-1}$) (Table 2). On the other hand, the endothermic peak corresponding to water melting around 0 °C was not observed, which indicated that freezable (available) water was not present in the film network (Hatakeyama & Hatakeyama, 1998). Unfreezable bound water is retained not only as the first layer of polymer hydration but also in the coordination sphere of calcium crosslinks (Braccini & Pérez, 2001; Ping, Nguyen, Chen, Zhou, & Ding, 2001).

3.2.2. Water vapor permeability (WVP)

The WVP calculated according to the ASTM E 96-80 (1987) cup method for synthetic polymers underestimates the WVP of hydrophilic edible films because neglects the resistance of the air column into the cup, between the film and the top of the anhydrous $CaCl_2$ bed. The WVP was then determined across a 0%/75% RH gradient, at 25.0 °C, and calculated by applying the correction of Gennadios et al. (1994) for hydrophilic edible films. Values of WVP between 1.3×10^{-9} and 1.6×10^{-9} $g\,m^{-1}\,s^{-1}\,Pa^{-1}$ were determined, with non significant difference between films (Table 2).

Huq et al. (2012) developed alginate (3.0% w/v in the film forming solution) based films without plasticizers, loaded with nanocrystalline cellulose (1–8% w/w on dry basis) and crosslinked by immersion of the casted films in a $CaCl_2$ solution (1% w/v). They determined the WVP at 25.0 °C across a 0%/60% RH gradient, through the ASTM 15.09:E96 method (1983). The authors found that the WVP decreased from 6.37×10^{-11} to 4.05×10^{-11} $g\,m^{-1}\,s^{-1}\,Pa^{-1}$ as the proportion of nanocrystalline cellulose in the film increased from 0% to 8%. Cellulose based nanoparticles are not as hydrophilic as the CF herein used, which include not only cellulose and lignin but also relevant proportions of pectins (≈15%) and hemicelluloses (≈30%) (Table 1). Also, in the present work, a lower LMP concentration (1.75% w/w in the film forming solution) than in the cited work was used.

3.2.3. Tensile tests

The normal stress (σ)–strain (ε) curves were recorded through tensile tests performed under controlled force until film fracture in a DMA, at low velocity of force increment (0.3 N/min). Certainly, the particle sizes of carrot fibers (53–210 μm) were well above pectin macromolecule sizes. Films could probably be particulate-polymer composites containing a filler with relatively small and variable aspect ratios.

Table 2
Physical properties[a,b] and antioxidant capacity[a,b,c] determined on low methoxyl pectin based films made without (0%-CF LMP) or with carrot fibers (CF) of different particle size. Kinetic parameters[a,b] of L-(+)-ascorbic acid (AA) decay and *b*-color parameter increase (k_b) in films, as well as the *a* and *b* color parameter values recorded at initial time of film storage at 25 °C and 57.7% relative humidity, are also summarized.

	0%-CF LMP film	Composite films: average particle size (μm)		
		53	105	210
Thickness (mm)	0.137 ± 0.005^{A}	0.160 ± 0.008^{B}	$0.162 \pm 0.006^{B,C}$	0.174 ± 0.009^{C}
Moisture content (g/100 g dm)	25.7 ± 0.4^{A}	25.2 ± 0.8^{A}	25.3 ± 0.4^{A}	25.8 ± 0.3^{A}
Glass transition temperature, T_g (C)	−68.49	−72.34	−71.37	−69.85
Change in specific heat at the glass transition[J/g(dm)K]	3.542	3.372	3.871	3.230
WVP × 10^9 (g m^{-1} s^{-1} Pa^{-1}) (25 °C; 0%/75%RH)	1.32 ± 0.04^{A}	1.35 ± 0.05^{A}	1.6 ± 0.3^{A}	1.6 ± 0.2^{A}
Contact angle (°) measured at 5 s	26 ± 4^{A}	20 ± 2^{B}	33 ± 9^{AC}	37 ± 8^{C}
Contact angle (°) measured at 60 s	21 ± 4^{A}	13 ± 1^{B}	28 ± 9^{A}	31 ± 9^{A}
DPPH[c] (mg AA/100 g film)	ND	ND	ND	ND
FRAP[c] (mg AA/100 g film)	ND	7.1 ± 0.9^{A}	5.3 ± 0.2^{B}	6 ± 1^{AB}
k'_{AA} × 10^6 (min^{-1})[d]	5.9 ± 0.2^{A}	4.3 ± 0.1^{B}	5.3 ± 0.2^{C}	6.0 ± 0.2^{A}
$t_{1/2}$ (d)[e]	82	111	91	80
a	−1.9	−0.6	+0.5	+1.0
b	+13.2	+13.0	+13.2	+13.2
b (Average value recorded during the period of storage)[a]	$+12.7 \pm 0.6^{A}$	$+19 \pm 3^{B}$	$+15 \pm 2^{C}$	$+16 \pm 2^{C}$

[a] Mean and standard deviations for $n = 3$ ($n \geq 12$ for *a*, *b* color parameters) are reported.
[b] The same capital letter as superscript of data in a given row means non significant differences ($p < 0.05$).
[c] Results of the DPPH and FRAP assays are expressed as L-(+)-ascorbic acid (AA), which was used as standard. dm: dry mass.
[d] Rate constant of AA hydrolysis.
[e] Half-life time of the AA loaded in films, expressed in days (d).
ND: non detectable.

All film systems were plasticized by glycerol at the same proportion with respect to the LMP polymer (76.2 g/100 g LMP) as well as by the same moisture content (Table 2). Fig. 3 shows the values of the elastic modulus E_C (Eq. (5)), modulus of rupture E_{rupt} (Eq. (8)) as well as the corresponding mean values of percent of strain (ε%) recorded at film rupture as a function of the CF average particle size. As expectable, the elastic modulus E_C was always higher than the modulus of rupture E_{rupt} for each kind of film (Fig. 3). It can be observed that, for different reasons, the elastic modulus E_C decreased significantly ($p < 0.05$) with the addition of CF, at all particle sizes studied, especially for 53 and 105 μm. The elastic modulus E_C increased with the particle size of the fiber filler (Fig. 3). At the same time, the relative elongation or strain (ε) at film rupture, expressed in percentage, decreased significantly ($p < 0.05$) by loading with the 53-μm CF, whereas the 105- and 210-μm particle fillers respectively produced the same relative elongation at film failure that LMP films without CF (Fig. 3). Hence, the composite film developed with 53 μm particle size of CF showed the lowest value of elastic modulus E_C because of the lowest corresponding values of true stress and true strain (Eq. (5)) obtained. Conversely, lower values of elastic modulus E_C showed by the 105-μm- and 210-μm-CF composites than the elastic modulus E_C of 0%-CF LMP film was due only to the lower values of stress recorded during the tensile assay, since the strain values were not different (Fig. 3). The mechanical performance of films was then dependent on the presence of CF as well as on the particle size of fibers. As denoted by the value of elastic modulus E_C, the 53-μm CF composite was the least elastic film, as well as the least deformable film (Fig. 3). On the other hand, the 105-μm- and 210-μm-CF composites were as deformable as the 0%-CF LMP film but less stiff (Fig. 3). The same conclusions can be drawn by comparing the values of the modulus of rupture (E_{rupt}) obtained, which refers to the film strength (Fig. 3). Above the glass transition temperature (Table 2), the crack propagation which culminates in rupture can be strongly influenced by the presence of filler particles (Ferry, 1980).

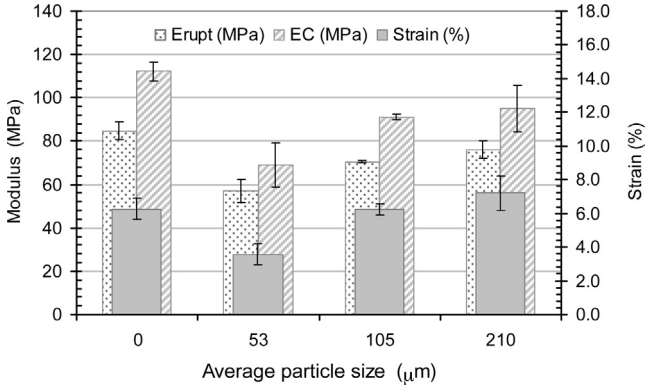

Fig. 3. Elastic modulus (E_C), modulus of rupture (E_{rupt}) and the strain (%) recorded at film failure are plotted against the carrot fiber particle size (μm). Error bars correspond to the standard deviation ($n \geq 4$).

The decrease in film elongation only observed in the case of 53-μm CF composite can be indicating some strong interaction of the 53 μm carrot fiber particles with the hydrophilic (compatible) LMP film network. Probably, it revealed that a new film matrix could have been formed, probably as a blend, which can need a proportion of plasticizer according to the total polymer content loaded (LMP + 53 μm-CF). Loading the films with the 105 μm particle size produced lower values of elastic modulus (E_C) and of the modulus of rupture (E_{rupt}) than in the case of the 0%-CF LMP-films due only to the decrease in the corresponding stress (σ_T or σ). The hydration level related to the particle size (Fig. 2a, b) reached by the fiber fillers during making of the film forming solution could be sufficient to permit the strongest physical interaction with the pectin macromolecules (LMP) during swelling in the aqueous film forming solution, where calcium was finally added for gelling before casting. Probably, each 53 μm CF particle may be bridged physically to others by many LMP polymer chains, and it acts as a multiple crosslink as well as a rigid occupier of space (Ferry, 1980). It allowed constituting a strengthened polymeric matrix by dehydration during the film casting process. This phenomenon did not occur in the case of the 210 μm of carrot fiber particle size. The important level of pectins found in the CF (Table 1) can also be hydrated and swelled in the film forming solution, then contributing to the film network development of composites.

3.2.4. Microscopy and contact angle

Atomic force microscopy (AFM) images (1 μm × 1 μm) were taken from films. This scale of image is actually lower than the fiber particle sizes used to the development of the composite films.

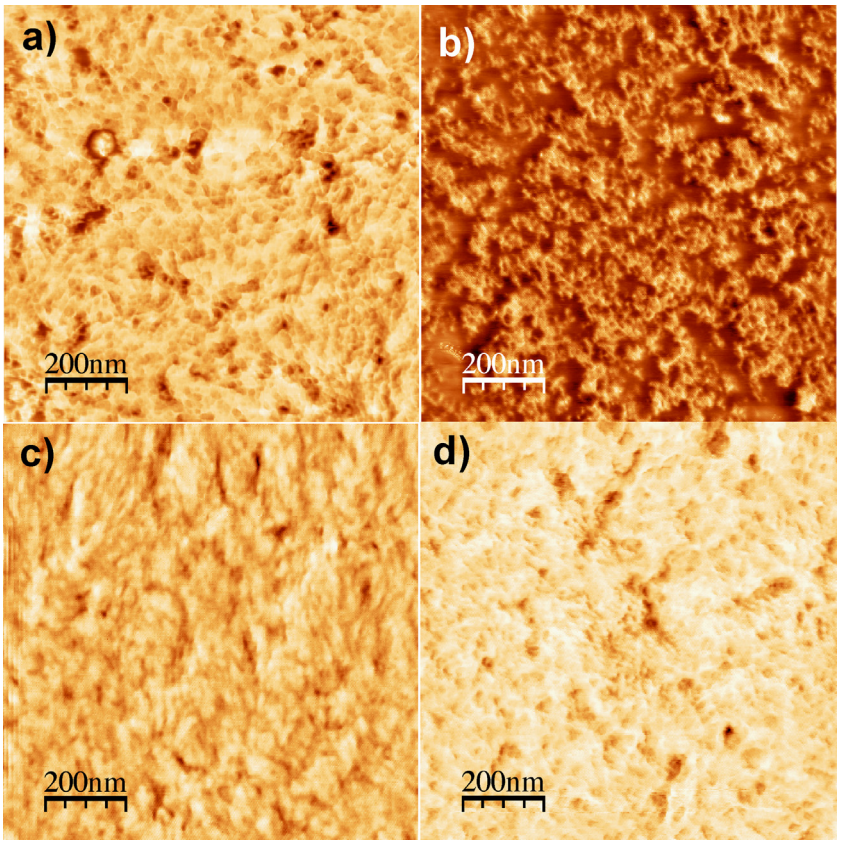

Fig. 4. Atomic force microscopy images (1 μm × 1 μm) of the LMP film (a) and composite films loaded with carrot fibers of 53 (b), 105 (c) or 210 μm (d) particle size.

However, it can be observed the aspect of the film nanostructure or if the polymeric nanostructural matrix was altered by the presence of CF. The 0%-CF-LMP film shows a quite uniform matrix of aggregated globular structures or flocks with diameters between 17 and 24 nm (Fig. 4a). This nanostructure in general underlies in the 53-μm carrot fiber composite film, though alternating with some smooth and flat areas (Fig. 4b). The flock-aggregated nanostructure of the LMP network seems to be distorted when loaded with 105-μm carrot fiber (Fig. 4c). The nanostructure of the 210 μm-fiber composite film is similar to that of the 0%-CF-LMP film (Fig. 4d).

The contact angle was also determined through the method of a sessile water drop deposited on the film surface that was in contact with the ambient during the drying process of casting (Table 2). Results are reported in Table 2. For the 0%-CF-LMP film and composites, the contact angle values obtained were well below 90° (20–37°) and hence, they are hydrophilic or wettable, as expectable. The values decreased after 60 s of sessile drop permanence on the film surface (Table 2).

3.2.5. *FTIR analysis of films*

Since the chemical composition of CF was not dependent on the particle size, the FTIR spectra of CF powders were not different. The FTIR analysis of CF performed by transmission showed the typical spectra of cell wall polymers (see 53 μm-fiber powder spectrum, Fig. 5). The broad typical band recorded at ≈3428 cm^{-1} of wavenumber is ascribed to intra and intermacromolecular hydrogen bondings of polysaccharides from cell walls (Coimbra, Barros, Barros, Rutledge, & Delgadillo, 1999), and the broad shorter band at 2935 cm^{-1} corresponds to the OH-stretching in the carboxylic groups observed in the FTIR spectra of CF (Fig. 5). The 1731 cm^{-1} band is attributed to the C=O stretching of the esterified carboxyl group of the pectinic (polygalacturonic acid) component, whereas the intensity of the broader band recorded at 1621 cm^{-1}, is ascribed to the C=O stretching of the unesterified carboxylic group of pectins. Also, an absorption at 1633 cm^{-1} is reported as principally associated with the adsorbed water (Fig. 5), since the hemicelluloses usually have a strong affinity for water and, in the solid state, these macromolecules may have disordered structures which can easily be hydrated (Chaikumpollert, Methacanon, & Suchiva, 2004). Similarly, the FTIR spectra of pectins can show a water deformation band at 1640 cm^{-1}, which corresponds to the water adsorbed (δ HOH) by pectins. Small bands at 1243, 1330 and 1423 cm^{-1} can be ascribed to the C—H stretch and CH or OH bending in hemicelluloses and celluloses (Fig. 5). The bands at 1379 and 1163 cm^{-1} can be respectively attributed to C—H deformation and C—O—C vibration in hemicelluloses and cellulose (Chaikumpollert et al., 2004). Between 1020 and 1170 cm^{-1} corresponds mainly to cellulose and hemicelluloses.

When CF particles were present in the LMP film network, the FTIR spectra obtained through attenuated total reflectance surface (ATR) corresponded only to the spectrum of the LMP plasticized by hydrogen-bounded glycerol and water (equilibration at 57.7% RH). This can be concluded when the spectra called "53 μm-CF" and "105 μm-CF composite film" are compared with the spectrum called "0%-CF LMP-film" (Fig. 5). Films made only with LMP and stored under anhydrous (0% RH) atmosphere (called "pure LMP film", Fig. 5) showed a similar spectrum with the characteristic bands of the polygalacturonic backbone in the fingerprint zone (1200 to 900–850 cm^{-1}), at 1020 (sharp band) and 1105 cm^{-1} (McCann, Hammouri, Wilson, Belton, & Roberts, 1992). Typical pectin bands were also present in this region corresponding to the C—H stretching in the carbohydrate backbone. Pectic samples are characterized mainly by the wavenumbers 1145, 1105, 1014 and 952 cm^{-1} (Coimbra et al., 1999), where 1105 and 1014 cm^{-1} bands are diagnostic wavenumbers of pectic polysaccharides rich in uronic acids. Some of these characteristic bands in the case of pectin

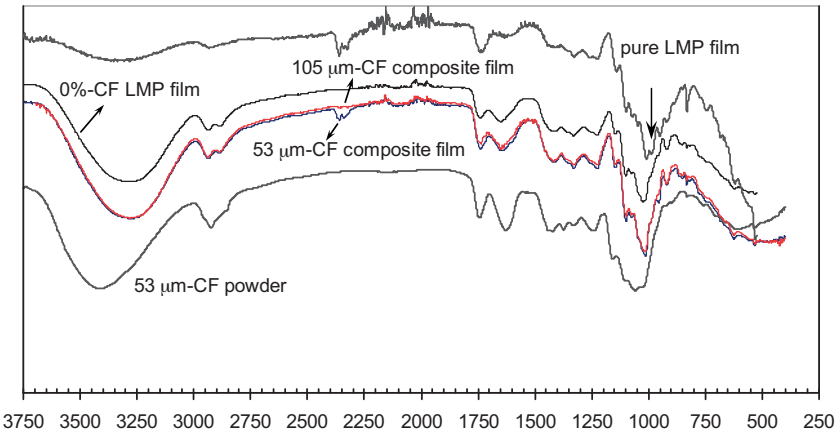

Fig. 5. FTIR spectra obtained from carrot fiber powder (53 μm) as well as from LMP and composite films.

film samples can be seen in Fig. 5, such as the asymmetric stretching of the glycosidic link at 1145 (Alonso-Simón, Encina, García-Angulo, Álvarez, & Acebes, 2004) and 1105 cm^{-1} (less intense), as well as signals at 1054 and 1060 cm^{-1}, a shoulder at 984 and lower intense bands at 962 and 925 cm^{-1} were also laterally observed ("pure LMP film", Fig. 5). When glycerol was added to the latter pectin film, it was remarkable to note the higher intensity of bands at 1105 cm^{-1} and 1020 cm^{-1} (Fig. 5). Indeed, the small peaks at 1054 and 1060 cm^{-1} (see "pure LMP film", Fig. 5-arrow) were completely masked in presence of glycerol by the broadening of the sharp band observed at 1020 cm^{-1}, due to hydrogen bonding (Fig. 5). A broad shorter band at 2945 cm^{-1} that corresponds to the OH-stretching in the carboxylic group and C—H stretching in the backbone, can be observed in the spectrum of the pure LMP film stored at 0% RH (Fig. 5). When glycerol was present, two bands appeared at 2898 and 2945 cm^{-1} which came from the C—H (saturated) stretching, characteristic of glycerol (Pérez et al., 2009).

All these results corroborated that the calcium crosslinked LMP network predominated at the composite film surfaces. Therefore, the LMP film (0%-CF) and the composite film spectra corresponded to the characteristic spectrum of the plasticized LMP film polymer (Fig. 5). As a consequence, the contact angle values measured at the film surface were, in general, similar among the different film systems at 5 s of contact (Table 2).

3.2.6. L-(+)-Ascorbic acid and carotene stability in films

The antioxidant activity determined in the films developed without the addition of AA is reported in Table 2. Radical scavenging activity (DPPH assay) was not detectable, whereas some reducing capability (FRAP assay) was determined in films containing CF. The latter was due to the proportion of CF present into each film sample.

Antioxidant property of films developed by addition of AA besides CF also depends in part on the half-life time of the AA loaded. The AA decays through hydrolysis when stored in the absence of oxygen, under vacuum (León & Rojas, 2007). At 57.7% of film equilibration, the water less adsorbed or less immobilized by the polymeric network is then available for chemical reactions (Labuza et al., 1972). Hence, the AA stability depended on the degree of water immobilization produced by the polymeric matrix of films as previously observed by León and Rojas (2007) in gellan films. The AA present in the equilibrated film network can also act as a tester of the water availability in the film matrix (León & Rojas, 2007). It was observed that the AA stability during storage in the absence of air, at constant temperature (25.0 °C) and RH (57.7%), was affected by the particle size of the CF used for composite film development. The AA decayed according to a pseudo-first order kinetic of reaction from the initial time of storage ($t = 0$) and the rate constant (k'_{AA}) was then calculated (Table 2). The highest AA stability was found in the composite films loaded with the 53 μm CF. The rate constants of AA destruction (k'_{AA}) increased significantly ($p < 0.05$) with the particle size of the CF, whereas in the absence of CF, the rate constant of AA decay was not different from that determined for 210 μm-CF loaded films (Table 2). The *a* color parameter of films recorded at initial time of storage, increased with the presence of fiber as well as with the average particle size (Table 2). However, the *b* values measured at initial time did not change with the presence of CF. Afterwards, the *b* color increased slightly but not significantly ($p < 0.05$) during film storage only when CF were present, as demonstrated through the *b*-values obtained by averaging the *b*-data recorded during the complete period of film storage performed for kinetic study (Table 2). The lowest average *b*-value and narrow standard deviation of data corresponded to the LMP-film without CF. The highest average *b*-value and wider standard deviation of data was obtained for the 53 μm-composites (+19; Table 2). Hence, carotenes of CF did not decay during film storage. Change in the *b*-value can be a direct manifestation of changes in carotenoid concentration (Ahmed, Shivhare, and Sandhu, 2002), particularly, of β-carotene (Dutta, Dutta, Raychaudhuri, and Chakraborty, 2006). It can be then suggested that CF may constitute a natural polymeric matrix for supporting of β-carotene in films.

The corresponding half-life times ($t_{1/2}$) of AA calculated (Eq. (9)) from the pseudo-first order rate constants (k'_{AA}) are also summarized in Table 2. As tested through the AA stabilization, it can then be inferred that the network constituted by the 53 μm carrot particles bridged by the LMP polymer chains may have contributed to the highest water immobilization.

4. Conclusions

Average particle sizes of 53, 105 and 210 μm of the hot water extracted CF, containing high amounts of bioactive compounds such as carotenoids (≈17.5 mg/100 g) and phenolics (≈235 mg GA/100 g) co-extracted with the polysaccharide component (80%), rich in pectins (15%), affected the hydration properties of CF. Consequently, the mechanical performance and antioxidant life-time (AA stability) of the LMP-based composites were also dependent on the particle size. It is suggested that the hydration properties of CF affected the film microstructure (mechanical properties) and water mobility (AA stability) in the polymeric matrix. The 53-μm CF showed the lowest hydration capability, producing the least stiff and deformable film due probably to the formed network constituted by CF particles bridged by the LMP chains acting as a multiple crosslink. The own pectins of CF can also contribute to the formation of the film microstructure in the case of 105 and

210 μm particle sizes, with higher hydration properties, but to a lesser extent in the case of 53 μm CF. The 53-μm-CF LMP-film matrix also produced the highest water immobilization and, hence, the highest stabilization of the AA loaded when films were stored at 57.7% RH and 25.0 °C under vacuum, in the darkness. Carotenes did not decay during film storage at 57.7% RH at 25 °C in presence of AA, being then suggested that CF can also constitute a natural polymeric matrix for supporting of carotenes in films. However, the presence of CF did not decrease the WVP of films because of the hydrophilic nature of the CF containing pectins. It is then important to consider the potential influence of the fiber particle size in the film performance when composites are developed for food preservation.

Acknowledgements

This work was supported by grants from University of Buenos Aires, National Research Council of Argentina (CONICET) and ANPCyT. We are also grateful to the SENESCYT (República del Ecuador) for the financial support of the Idrovo Encalada's fellowship. We are also grateful to Carlos Rozas (INTI-Celulosa y Papel, Argentina) for the goniometer use for contact angle, as well as to CP-Kelco (Denmark) for providing the pectin.

References

Abdollahi, M., Alboofetileh, M., Rezaei, M., & Behrooz, R. (2013). Comparing physico-mechanical and thermal properties of alginate nanocomposite films reinforced with organic and/or inorganic nanofillers. *Food Hydrocolloids*, *32*, 416–424.

Ahmed, J., Shivhare, U. S., & Sandhu, K. S. (2002). Thermal degradation kinetics of carotenoids and visual color of papaya puree. *Food Engineering and Physical Properties*, *67*(7), 2692–2695.

Alonso-Simón, A., Encina, A. E., García-Angulo, P., Álvarez, J. M., & Acebes, J. L. (2004). FTIR spectroscopy monitoring of cell wall modifications during the habituation of bean (*Phaseolus vulgaris* L.) callus cultures to dichlobenil. *Plant Science*, *167*(6), 1273–1281.

ASTME 96-80. (1987). ASTM (1987). Standard methods for water vapor transmission of materials (E 96-80). In *Annual book of ASTM standards*. Philadelphia, PA: American Society for Testing and Materials.

ASTM. (1983). *Method 15.09:E96. Standard test method for water vapor transmission of materials*. Philadelphia, PA: American Society for Testing and Materials.

Azeredo, H. M. C., Miranda, K. W. E., Rosa, M. F., Nascimento, D. M., & de Moura, M. R. (2012). Edible films from alginate–acerola puree reinforced with cellulose whiskers. *LWT – Food Science and Technology*, *46*, 294–297.

Basanta, M. F., de Escalada Pla, M. F., Stortz, C. A., & Rojas, A. M. (2013). Chemical and functional properties of cell wall polymers from two cherry varieties at two developmental stages. *Carbohydrate Polymers*, *92*, 830–841.

Benzie, I. F. F., & Strain, J. J. (1996). The ferric reducing ability of plasma (FRAP) as a measure of "antioxidant power": The FRAP assay. *Analytical Biochemistry*, *239*, 70–76.

Biswas, A. K., Sahoo, J., & Chatli, M. K. (2011). A simple UV–Vis spectrophotometric method for determination of β-carotene content in raw carrot, sweet potato and supplemented chicken meat nuggets. *LWT – Food Science and Technology*, *44*, 1809–1813.

Braccini, I., & Pérez, S. (2001). Molecular basis of Ca^{2+}-induced gelation in alginates and pectins: The egg-box model revisited. *Biomacromolecules*, *2*, 1089–1096.

Brand-Williams, W., Cuvelier, M. E., & Berset, C. (1995). Use of free radical method to evaluate antioxidant activity. *LWT – Food Science and Technology*, *28*, 25–30.

Brett, C. T., & Waldron, K. W. (1996). *The physiology and biochemistry of plant cell walls* (2nd ed., pp. 26–32). London, UK: Chapman & Hall.

Cadden, A. M. (1987). Comparative effects of particle size reduction on physical structure and water binding properties of several plant fibers. *Journal of Food Science*, *52*, 595–599.

Chaikumpollert, O., Methacanon, P., & Suchiva, K. (2004). Structural elucidation of hemicelluloses from Vetiver grass. *Carbohydrate Polymers*, *57*, 191–196.

Chau, C. F., Wang, Y. T., & Wen, Y. L. (2007). Different micronization methods significantly improve the functionality of carrot insoluble fibre. *Food Chemistry*, *100*, 1402–1408.

Coimbra, M. A., Barros, A., Barros, M., Rutledge, D. N., & Delgadillo, I. (1999). FTIR spectroscopy as a tool for the analysis of olive pulp cell-wall polysaccharide extracts. *Carbohydrate Research*, *317*, 145–154.

de Escalada Pla, M. F., Uribe, M., Fissore, E. N., Gerschenson, L. N., & Rojas, A. M. (2010). Influence of the isolation procedure on the characteristics of fiber-rich products obtained from quince wastes. *Journal of Food Engineering*, *96*(2), 239–248.

De'Nobili, M. D., Curto, L. M., Delfino, J. M., Soria, M., Fissore, E. N., & Rojas, A. M. (2013). Performance of alginate films for retention of L-(+)-ascorbic acid. *International Journal of Pharmaceutics*, *450*, 95–103.

De'Nobili, M. D., Pérez, C. D., Navarro, D. A., Stortz, C. A., & Rojas, A. M. (2013). Hydrolytic stability of L-(+)-ascorbic acid in low methoxyl pectin films with potential antioxidant activity at food interfaces. *Food and Bioprocess Technology*, *6*, 186–197.

De'Nobili, M. D., Rojas, A. M., Abrami, M., Lapasin, R., & Grassi, M. (2015). Structure characterisation by means of rheological and NMR experiments as a first necessary approach to study the L-(+)-ascorbic acid diffusion from pectin and pectin/alginate films to agar hydrogels that mimic food materials. *Journal of Food Engineering*, *165*, 82–92.

Del Nobile, M. A., Chillo, S., Falcone, P. M., Laverse, J., Pati, S., & Baiano, A. (2007). Textural changes of Canestrello Pugliese cheese measured during storage. *Journal of Food Engineering*, *83*, 621–628.

Dutta, D., Dutta, A., Raychaudhuri, U., & Chakraborty, R. (2006). Rheological characteristics and thermal degradation kinetics of beta-carotene in pumpkin puree. *Journal of Food Engineering*, *76*, 538–546.

Ferry, J. D. (1980). *Viscoelastic properties of polymers* (2nd ed., pp. 356–359). New York, USA: John Wiley & Sons., 426–433, 583.

Frias, J., Peñas, E., Ullate, M., & Vidal-Valverde, C. (2010). Influence of drying by convective air dryer or power ultrasound on the vitamin c and β-carotene content of carrots. *Journal of Agriculture and Food Chemistry*, *58*, 10539–10544.

Gennadios, A., Weller, C. L., & Gooding, C. H. (1994). Measurement errors in water vapor permeability of highly permeable, hydrophilic edible films. *Journal of Food Engineering*, *21*, 395–409.

Gordon, M. H. (2001). The development of oxidative rancidity in foods. In J. Pokorny, N. Yanishlieva, & M. Gordon (Eds.), *Antioxidants in food* (p. 17). Cambridge, UK: Woodhead Publishing Limited.

Greenspan, L. (1977). Humidity fixed points of binary saturated aqueous solutions. *Journal of Research of the National Bureau of Standards*, *81A*(1), 89–96.

Hashimoto, T., & Nagayama, T. (2004). Chemical composition of ready-to-eat fresh carrot. *Journal of the Food Hygienic Society of Japan*, *39*, 324–328.

Hatakeyama, H., & Hatakeyama, T. (1998). Interaction between water and hydrophilic polymers. *Thermochimica Acta*, *308*, 3–22.

Horcas, I., Fernandez, R., Gomez-Rodriguez, J. M., & Colchero, J. (2007). WSXM: A software for scanning probe microscopy and a tool for nanotechnology. *Review of Scientific Instruments*, *78*, 013705.

Huq, T., Salmieri, S., Khan, A., Khan, R. A., Le Tien, C., Riedl, B., et al. (2012). Nanocrystalline cellulose (NCC) reinforced alginate based biodegradable nanocomposite film. *Carbohydrate Polymers*, *90*, 1757–1763.

Karkalas, J. J. (1985). An improved enzymic method for the determination of native and modified starch. *Journal of the Science of Food and Agriculture*, *36*, 1019–1027.

Labuza, T. P., McNally, L., Gallagher, D., Hawkes, J., & Hurtado, F. (1972). Stability of intermediate moisture foods. 1. Lipid oxidation. *Journal of Food science*, *37*, 154–159.

León, P. G., Chillo, S., Conte, A., Gerschenson, L. N., Del Nobile, M. A., & Rojas, A. M. (2009). Rheological characterization of deacylated/acylated gellan films carrying L-(+)-ascorbic acid. *Food Hydrocolloids*, *23*, 1660–1669.

León, P. G., & Rojas, A. M. (2007). Gellan gum films as carriers of L-(+)-ascorbic acid. *Food Research International*, *40*, 565–575.

Mancini, M., Moresi, M., & Rancini, R. (1999). Mechanical properties of alginate gels: Empirical characterization. *Journal of Food Engineering*, *39*, 369–378.

McCann, M. C., Hammouri, M., Wilson, R., Belton, P., & Roberts, K. (1992). Fourier transform infrared microspectroscopy is a new way to look at plant cell walls. *Plant Physiology*, *100*(4), 1940–1947.

Ministerio de Agricultura, Ganadería, Industria y Comercio de la Provincia de Santa Fe, & Aimaretti, N. (1999). *Santa Fe, el mejor lugar del MERCOSUR para invertir*. Gobierno de la Provincia de Santa Fe: Santa Fe.

Oviasogie, O. P., Okoro, D., & Ndiokwere, C. L. (2009). Determination of total phenolic amount of some edible fruits and vegetables. *African Journal of Biotechnology*, *8*, 2819–2820.

Pérez, C. D., Flores, S. K., Marangoni, A. G., Gerschenson, L. N., & Rojas, A. M. (2009). Development of a high methoxyl-pectin edible film for retention of L-(+)-ascorbic acid. *Journal of Agricultural and Food Chemistry*, *57*, 6844–6855.

Ping, Z. H., Nguyen, Q. T., Chen, S. M., Zhou, J. Q., & Ding, Y. D. (2001). States of water in different hydrophilic polymers – DSC and FTIR studies. *Polymer*, *42*, 8461–8467.

Pulido, R., Bravo, L., & Saura-Calixto, F. (2000). Antioxidant activity of dietary polyphenols as determined by a modified FRAP assay. *Journal of Agriculture and Food Chemistry*, *48*, 3396–3402.

Rhagavendra, S. N., Rastogi, N. K., Raghavarao, K. S. M. S., & Tharanathan, R. N. (2004). Dietary fiber from coconut residue: Effects of different treatments and particle size on the hydration properties. *European Food Research and Technology*, *218*, 563–567.

Rojas-Graü, M. A., Avena-Bustillos, R. J., Olsen, C. O., Friedman, M. F., Martin-Belloso, O., Pan, Z., et al. (2007). Effects of plant essential oils and oil compounds on mechanical, barrier and antimicrobial properties of alginate–apple puree edible films. *Journal of Food Engineering*, *81*, 634–641.

Ritger, P. L., & Peppas, N. A. (1987). A simple equation for description of solute release. I. Fickian and non-Fickian release from nonswellable devices in the form of slabs, spheres, cylinders or discs. *Journal of Controlled Release*, *5*, 23–36.

Sánchez, O., & Cardona, C. (2008). Trends in biotechnological production of fuel ethanol from different feedstocks. *Bioresource Technology*, *99*, 5270–5295.
Scheller, H. V., & Ulvskov, P. (2010). Hemicelluloses. *Annual Review of Plant Biology*, *61*, 263–289.
Sharma, K. D., Karki, S., Thakur, N. S., & Attri, S. (2012). Chemical composition, functional properties and processing of carrot – a review. *Journal of Food Science and Technology*, *49*(1), 22–32.
Sirviö, J. A., Kolehmainen, A., Liimatainen, H., Niinimäki, J., & Hormi, O. E. O. (2014). Biocomposite cellulose–alginate films: Promising packaging materials. *Food Chemistry*, *151*, 343–351.
Sokal, R. R., & Rohlf, J. B. (2000). *Biometry: The principles and practice of statistics in biological research*. San Francisco: W.H. Freeman and Company.
Trezza, T. A., & Krochta, J. M. (2000). Color stability of edible coatings during prolonged storage. *Journal of Food Science*, *65*(1), 1166–1169.
Valencia-Chamorro, S. A., Palou, L., del Río, M. A., & Pérez-Gago, M. B. (2011). Antimicrobial edible films and coatings for fresh and minimally processed fruits and vegetables: A review. *Critical Reviews in Food Science and Nutrition*, *51*(9), 872–900.
van Holst, G. J., & Varner, J. E. (1984). Reinforced polyproline II conformation in a hydroxyproline-rich cell wall glycoprotein from carrot root. *Plant Physiology*, *74*(2), 247–251.
Vetter, S., & Kunzek, H. (2003). The influence of suspension solution conditions on the rehydration of apple cell wall material. *European Food Research and Technology*, *216*, 39–45.
Vincken, J. P., Schols, H. A., Oomen, R. J. F. J., McCann, M. C., Ulvskov, P., Voragen, A. G. J., et al. (2003). If homogalacturonan were a side chain of rhamnogalacturonan I. Implications for cell wall architecture. *Plant Physiology*, *132*, 1781–1789.
Waldron, K. W., Smith, A. C., Parr, A. J., Ng, A., & Parker, M. (1997). New approaches to understanding and controlling cell separation in relation to fruit and vegetable texture. *Trends in Food Science and Technology*, *8*, 213–221.